



Cite this: *RSC Adv.*, 2022, 12, 1157

Highly sensitive, room temperature operated gold nanowire-based humidity sensor: adoptable for breath sensing

Parag V. Adhyapak, * Aishwarya M. Kasabe, Amruta D. Bang, Jalindar Ambekar and Sulabha K. Kulkarni

A novel, highly sensitive gold nanowire (AuNW) resistive sensor is reported here for humidity sensing in the relative humidity range of 11% to 92% RH as well as for breath sensing. Both humidity and breath sensors are widely needed. Despite a lot of research on humidity and breath sensors, there is a need for simple, inexpensive, reliable, sensitive and selective sensors, which will operate at room temperature. Here we have synthesized gold nanowires by a simple, wet chemical route. The nanowires synthesized by us are 4–7 nm in diameter and a few micrometers long. The nanowires are amine functionalized. The sensor was prepared by drop casting gold nanowires on an alumina substrate to form a AuNW layer with different thicknesses (10, 20, 30 μm). The AuNW sensor is highly selective towards humidity and shows minimum cross sensitivity towards other gases and organic vapors. At an optimum thickness of 20 μm , the humidity sensing performance of the AuNW sensor over 11% to 92% RH was found to be superior to that of 10 and 30 μm thick layers. The response time of the sensor is found to be 0.2 s and the recovery time is 0.3 s. The response of the AuNW sensor was 3.3 $\text{M}\Omega/\%$ RH. Further, the AuNW sensor was tested for sensing human breathing patterns.

Received 11th October 2021
Accepted 6th December 2021

DOI: 10.1039/d1ra07510a

rsc.li/rsc-advances

1. Introduction

Amongst the various nanostructured materials, gold metal nanostructures have attracted great attention due to their interesting and enhanced optical, catalytic and electronic properties.^{1–5} In ancient times, gold was used in making glass for decorative purposes, without knowing how it produced attractive magenta, pink, red and other colors depending on its processing. Now it is known that the particle size and shape, leading to different spectral positions of surface plasmon resonance are responsible for these exotic optical properties. Gold is well known for its non-interactive nature, but at the nanoscale it enables surface interactions. Research in the 20th and 21st century has led to better understanding and use of gold nanostructures in areas like biosensors, gas sensors, drug delivery, tissue welding, photo therapy and so on.^{6–12} Conventionally, metal oxides like doped SnO_2 , ZnO *etc.* are considered to be good humidity sensors. There are a variety of ways of humidity sensing *viz.* gravimetric, capacitive, resistive, magnetoelastic methods *etc.* which have been reviewed earlier.^{6,13,14} However, in the last few years gold nanostructures have emerged as alternative sensors because of their operation at low temperatures.^{7,9} Our group also has reported recently use of bimetallic core-shell resistors in humidity sensing.¹⁵ Humidity

sensors are required in hospitals, air conditioners, automobiles, research laboratories, space vehicles and many other areas. They are also required for agricultural use like food packaging, testing of soil moisture or green house maintenance.^{6,13,14} Zaihua Duan *et al.*¹⁶ have recently fabricated a halloysite nanotube based sensor for humidity sensing in the range of 7.2–91.5% RH. Shaukat *et al.*¹⁷ have demonstrated a highly sensitive TiSi_2 based humidity sensor with all range linear humidity sensing performance. Yanyi Huang *et al.*¹⁸ have used halide perovskites as potential humidity-detection materials due to their sensitivity to water. Here lead-free $\text{Cs}_3\text{Cu}_2\text{Br}_5$ perovskite microcrystals are used to prepare an environmentally friendly humidity sensor.

Although many humidity sensors are available, still there is a lack of highly sensitive, inexpensive and reliable humidity sensor, which is still a driving force in search of new materials for humidity sensors.

Our efforts in search of humidity sensor show that gold nanowires (AuNW) are highly sensitive, selective, stable, covering large range (11% to 92%) of humidity. Electrochemical, optical humidity sensors based on AuNW have been reported earlier but resistive AuNW humidity sensors are not reported. AuNWs have a large surface to volume ratio due to their large aspect ratio *viz.* large length (few μm) to diameter (few nm). Moreover, AuNW are able to make a very well network, which can increase their overall conductance. The resistive sensors are much easier to operate, portable and user friendly

Centre for Materials for Electronics Technology (C-MET), Panchawati Off Pashan Road, Pune –411008, India. E-mail: adhyapak@cmet.gov.in; adhyapakp@yahoo.com



compared to other types of sensors. Moreover, the sensor we propose here is operated at room temperature, which is another cost reducing factor, making it more useful. Further, we have demonstrated it as a breath sensor. The idea of using it as a breath sensor is based on the fact that humans exhale ~5 to 6% (by volume) water vapor while breathing. Therefore, the material sensitive towards humidity easily works as a good breath sensor/analyzer.¹⁹ Moreover, if they are compact they can be portable and useful as wearable device. Breath analyzers are useful in health monitoring as breath patterns are indicators of health. Therefore, wearable compact breath analyzers need to be developed. Recently, breath analyzers using ink jet printed gold nanoparticle and gold aerogel sensors have also been reported.^{20,21} Nevertheless, the gold nanowire-based sensor proposed here is more sensitive and easier to fabricate.

2. Experimental

2.1 Materials

Gold chloride ($\text{HAuCl}_4 \cdot \text{H}_2\text{O}$), oleylamine (OA) ($\text{C}_{18}\text{H}_{37}\text{N}$), hexane (C_6H_{14}), triisopropylsilane (TIPS) ($\text{C}_9\text{H}_{22}\text{Si}$) from Sigma Aldrich and deionized (DI) water were used in this synthesis of AuNW.

2.2 Synthesis procedure

AuNWs were synthesized using a very simple wet chemical method.²² In this one step procedure 3 mg of gold chloride was added to 2.5 mL hexane. Further 100 μL oleylamine and 150 μL triisopropylsilane ($\text{C}_9\text{H}_{22}\text{Si}$) were added to it. A yellow colored solution was obtained. This solution was left undisturbed for 12 hours at room temperature which turns into dark red color. The resultant product was centrifuged and washed three times with ethanol to remove excess oleylamine and re-dispersed in hexane. Final product is oleylamine capped gold nanowires (AuNW).

2.3 Characterization

The obtained AuNW have been characterized by using various characterization techniques. UV-Visible analysis was performed using Jasco V-570 spectrometer. The AuNW solution was placed in a quartz cuvette and the optical spectrum was then recorded in the 400 to 800 nm range.

The morphology of the AuNW sample was investigated using a Field Emission scanning electron microscope (FESEM) JEOL-Hitachi S-4800F. The sample was prepared as follows; a drop of AuNW solution was placed on the Si substrate and dried. The substrate was inserted in the vacuum chamber of the FESEM held at $\sim 10^{-8}$ mbar vacuum.

The structural analysis was performed using X-ray diffraction analysis. Rigaku Miniflex X-ray diffractometer equipped with copper target ($\text{CuK}\alpha_1$, $\lambda = 1.5406 \text{ \AA}$) using nickel filter was used for the analysis. Few drops of AuNW liquid sample were allowed to dry on the glass substrate used for the XRD analysis. The diffraction pattern was recorded from $2\theta - 20^\circ$ to 60° angular range.

FTIR analysis of AuNW liquid sample in the spectral range from 400 to 4000 cm^{-1} was carried out using a Bruker TENSOR37 spectrometer.

2.4 Humidity sensing

For measurement of humidity sensing performance, AuNW were coated on interdigitated electrodes (IDE) using drop-casting method (Fig. 1(a)). The IDE is made up of alumina substrate with silver patterns on it. The thickness of the coating layer was varied as 10, 20 and 30 micron. The IDE was then connected to Keithley digital multimeter (DMM 7510) to measure the change in resistance. The humidity sensing performance was measured in air tight controlled humidity chambers containing 50 mL standard supersaturated solutions with respective specific relative humidity, KNO_3 (92% RH), KCl (84% RH), NaCl (75% RH), NH_4NO_3 (62% RH), $\text{Ca}(\text{NO}_3)_2 \cdot 4\text{H}_2\text{O}$ (51% RH), $\text{MgCl}_2 \cdot 6\text{H}_2\text{O}$ (33% RH) and LiCl , (11% RH). The chambers with standard solution were kept air-tight for 24 h to attain the equilibrium. For measurement of humidity performance, the sample was exposed to each chamber and resultant change in resistance was recorded on digital multimeter at room temperature ($\sim 30^\circ \text{C}$). The chamber exchange process was done within fraction of seconds to avoid the exposure of sample to outside environment.

For breathing analysis, the IDE was fitted inside the mask (as shown in Fig. 1(b)) and connected to the digital multimeter. The breathing patterns were obtained by exhaling and inhaling over the sample.

3. Results and discussion

There are several methods by which AuNW with desired shapes can be produced. Particle assembly, hydrothermal method, template assistance or physical deposition are some of the common methods to synthesize gold nanowires.^{23–27} However, these methods have several disadvantages. Lengthy reaction time, high temperature treatment, complicated steps, poor morphology of the produced nanowires are some of these problems. Using the single step procedure, following ref. 22, we could obtain AuNWs.

In Fig. 2(a) UV-Vis spectrum of AuNW solution along with the actual photograph of as-prepared sample (inset) is shown. The

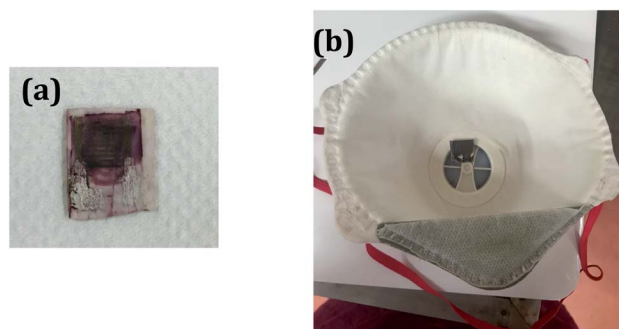


Fig. 1 (a) AuNW coated IDE (b) AuNW coated IDE fitted inside mask.



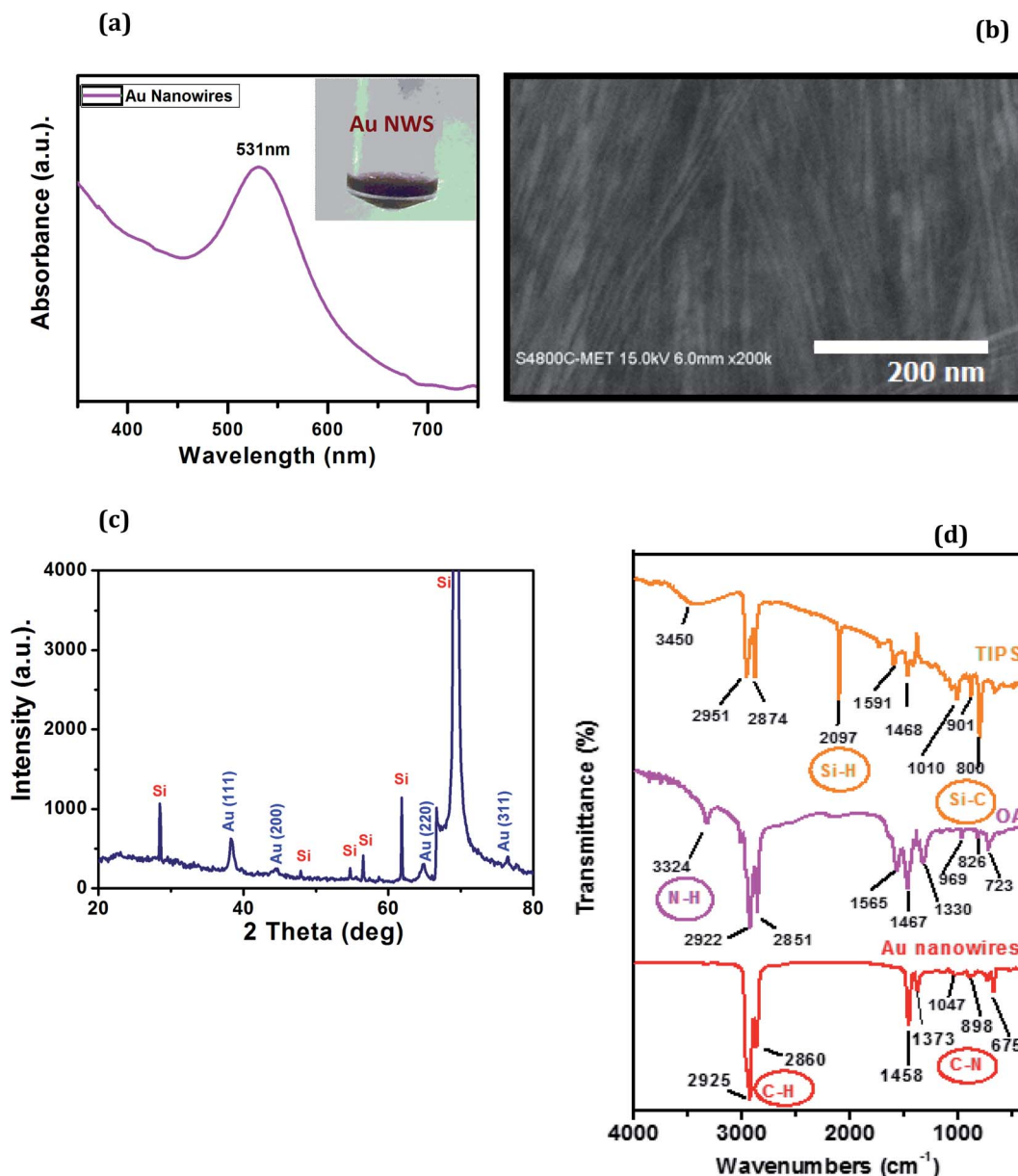


Fig. 2 (a) UV-Visible spectrum (b) FESEM image (c) XRD pattern of AuNW (d) FTIR spectra of TIPS, OA and AuNW.

solution has a dark magenta color and the spectrum shows a single peak located at ~ 531 nm, which is matching with the reported literature.²⁸ Morphology of the sample can be seen from FESEM in Fig. 2(b). The AuNW have a high aspect ratio. The diameters of the AuNW varied from ~ 4 to 7 nm *i.e.* average diameter was ~ 5.5 nm and lengths were 1.5 μm making an aspect ratio of ~ 300 . The wires were also found to be crystalline as is evident from the XRD analysis. Fig. 2(c) depicts the X-ray Diffraction pattern of amine coated gold nanowires of extremely high aspect ratio. One can notice four characteristic peaks at $2\theta = 38.36^\circ$, 44.48° , 64.82° and 76.44° corresponding to (100), (200), (220) and (311) diffraction planes respectively and can be attributed to FCC structure of gold which is in agreement with the JCPDS card #04-0784. The other peaks are due to Si substrate. Apart from these no other impurity peaks are observed in the XRD. Fig. 2(d) depicts the FTIR spectrum of the

AuNW sample along with that of capping molecule *viz.* oleylamine and TIPS as reference and used in the synthesis. Oleylamine has peaks at 3324 cm^{-1} due to N-H stretching, at 2922 and 2851 cm^{-1} due to asymmetric and symmetric C-H stretching. Peaks at 1565 and 723 cm^{-1} are due to N-H bending and C-C bending modes. Band at 969 is due to N-H bending vibrations. Similarly, TIPS show major characteristic peaks at 3450 cm^{-1} due to O-H stretching, at 2951 and 2874 cm^{-1} due to asymmetric and symmetric C-H stretching and at 2097 cm^{-1} due to Si-H, and at 800 cm^{-1} due to Si-C. In case of AuNW sample shows peaks at 2925 and 2860 cm^{-1} due to asymmetric and symmetric C-H stretching. Peak at 1458 cm^{-1} is due to $-\text{CH}_3$ bending vibrations. The peak at 1047 cm^{-1} is due to C-N bending vibrations, which is found shifted as compared to oleylamine. Thus, FTIR confirms the absence of TIPS and presence of oleylamine on the gold surface. These



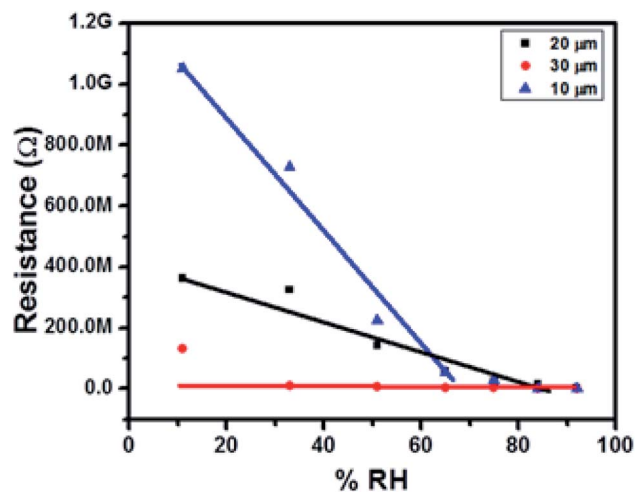


Fig. 3 Relation between resistance and relative humidity (% RH) for AuNW with different thicknesses.

identifications of TIPS and oleylamine on AuNW were also reported earlier in similar synthesis of AuNW.²²

We now proceed to show the results for the measurement of the relative humidity on AuNW samples.

We investigated the effect of AuNW coating thickness on the humidity response. Fig. 3 shows a plot of resistance against Relative humidity for 10, 20 and 30 μm thick AuNW layer. In case of AuNWs due to surfactants used in their synthesis to avoid the lateral growth (oleylamine in this case), the resistance of the AuNW sample can be rather high. This can be seen from the thickness dependent resistance of the devices fabricated here. It can be seen that, as the thickness increased from initial 10 μm to 20 μm , the resistance dropped from $\sim 1\text{ G}\Omega$ to 300 $\text{M}\Omega$ and further to 100 $\text{M}\Omega$ at 30 μm thickness of AuNW. This can be attributed to the increased end to end contact of AuNW.

We can conclude that with increase in the layers of gold nanowires, thickness of the AuNW coating increases providing more contacts in between the nanowires, which results in fast conduction through the material and reduction in the resistance. However, at 20 μm thickness the change in resistance with respect to humidity is distinctly measurable and ideal for device fabrication. Thus, we have performed further experiments with 20 μm thick AuNW material coating.

We further tried to find out the effect of humidification and dehumidification on the above three AuNW coatings. Here we have plotted the humidification and the dehumidification

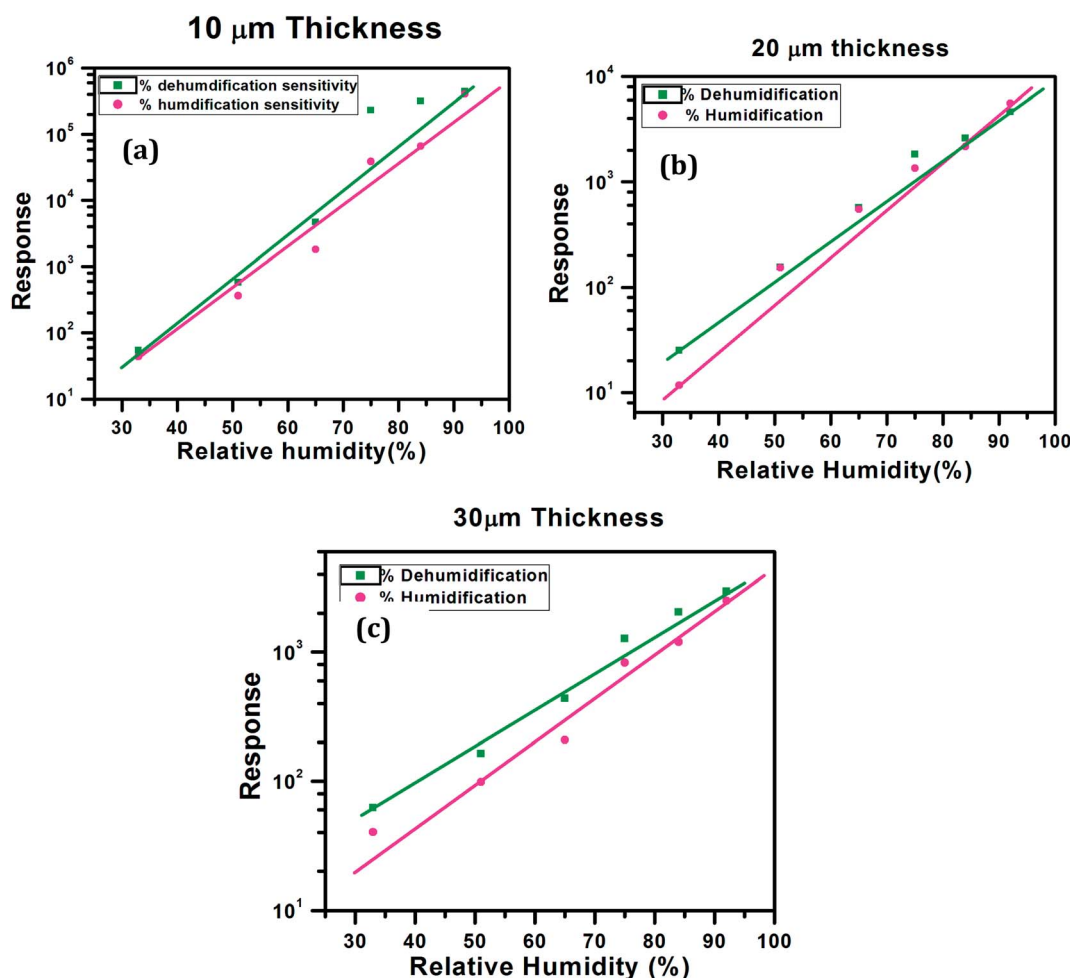


Fig. 4 Response as a variation of relative humidity (RH%) for three different thicknesses of AuNWs.



sensitivity at different humidity (see Fig. 4), the sensitivity is obtained by using the following formula (shown in eqn (1))

$$S\% = \frac{R_2 - R_1}{R_1} \times 100 \quad (1)$$

where, R_2 : new resistance after change in humidity R_1 : original resistance.

In each case, the response increases with relative humidity almost linearly with similar slopes but dehumidification shows a hysteresis for 10 and 30 μm AuNW coating. The best result in this case is for 20 μm AuNW coating, the humidification and dehumidification sensitivities are more linear. Therefore 20 μm thickness was considered to be optimum and further experiments were conducted using 20 μm thick AuNW coating.

The obtained results are better than the results reported for carbon nanotube/polymide composite films by Yoo *et al.* and recently by Ag ink by Barmpakos *et al.*^{29,30} Recently a 3-D porous network of gold nanoparticles chemically interconnected by dithiolated ethylene glycol oligomers was proposed as a humidity sensor.³¹ Although interesting due to high response and recovery time of few milliseconds, the response of the material is very low up to $\sim 70\%$ RH. On the other hand, our material has a very large resistance change or response (3.5 $\text{M}\Omega/\%$ RH) over the entire range of $\sim 11\%$ to 92% RH.

In Fig. 5(a) we have shown the graphs of change in resistance of the material with respect to humidity, with humidity ranging

from 11% RH to 92% RH. 10 cycles are shown depicting the repeatability of the material. The sample thickness was $20\text{ }\mu\text{m}$. As the humidity increases the resistance drops from $370\text{ M}\Omega$ to $9\text{ M}\Omega$ vary rapidly. In Fig. 5(b) one such cycle is shown separately for detail observation. The cycle represents sharp change in the resistance during humidification and dehumidification process. The response and recovery time values are quite shorter.

From Fig. 5(c) and (d) it can be noticed that $\Delta\text{RH} = 81\%$. Here for $\Delta\text{RH} = 81\%$ response time is 222 ms and recovery time is 308 ms . This can be compared with recent work in humidity sensing using inkjet orienting of gold nanoparticles.²⁰ The authors report response time of less than 1.2 s and recovery time of 3 seconds between $\Delta\text{RH} = 35.1\%$ whereas in the present work the response and recovery time is 0.2 s and 0.3 s for $\Delta\text{RH} = 81\%$. So ten times less response and recovery time has been achieved for wider range of humidity change.

We have also studied the dynamic response of the material for various humidity values. The response is as shown in Fig. 6 Here we can see that the material respond to various humidity levels. As humidity increases the resistance of the material decreases and *vice versa*. The outside humidity was around 40% RH when we conducted the experiments. Therefore, when the sensor was shifted from outside environment (40% RH) to the chamber with 11% and 33% RH humidity values, the resistance

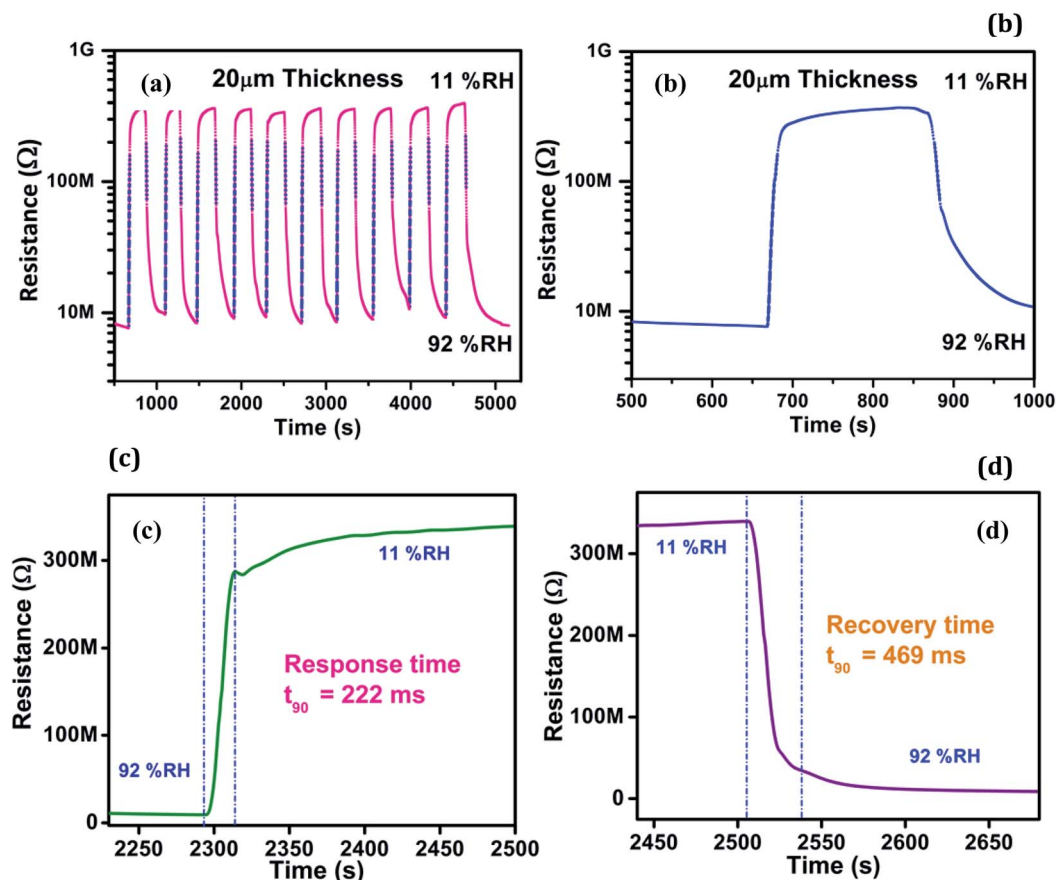


Fig. 5 (a) Change in resistance with respect to humidity for $20\text{ }\mu\text{m}$ thick AuNW film coated on IDE (10 cycles) (b) single cycle (c) response time curve and (d) recovery time curve.



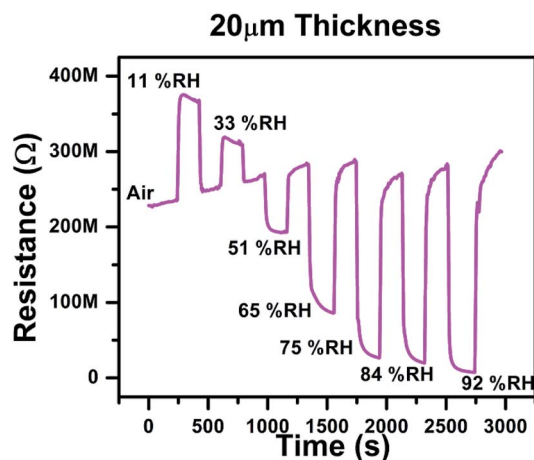


Fig. 6 Dynamic response of 20 μm thick AuNW for various humidity values.

was found to be increased. Similarly, when the sensor was shifted to the chambers with higher humidity values (higher than ambient humidity *i.e.* 40% RH), the resistance was found

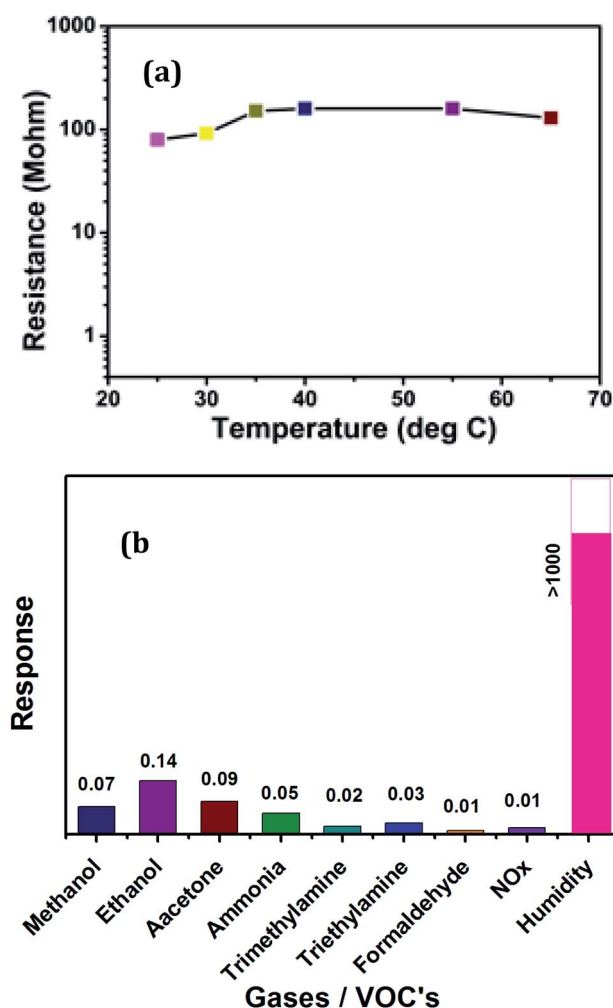


Fig. 7 (a) Temperature dependence of resistance for 20 μm thick AuNW (b) Response of AuNWs towards other gases and VOC's when compared with humidity.

to be decreased. These results are in accordance with our proposed mechanism.

We also investigated the effect of temperature on resistance for 20 μm thick AuNW coating. The resistance also depends on the humidity of the ambient. The initial resistance was 80 M Ω , as shown in Fig. 7(a). When the measurements were carried out in the range of 25 $^{\circ}\text{C}$ to 65 $^{\circ}\text{C}$, the resistance changes to 110 M Ω . Thus overall variation in the resistance is 20 M Ω , which is practically not much when compared with the overall change in the resistance in response to humidity *i.e.* from 300 M Ω to 9 M Ω .

We have also investigated the response of fabricated sensor towards other gases and organic vapors such as methanol, ethanol, acetone, ammonia, trimethylamine, triethylamine, formaldehyde and NO_x and the results are displayed in Fig. 7(b). It is observed that the sensor shows negligible response of less than 0.2 when compared with humidity which is >1000.

Due to high response of the AuNW towards humidity, we tried it for the breathing analysis. Humans are known to exhale ~5–6% (v) water vapor in each breath cycle. Therefore, we expected that the humidity sensor fabricated here could work as a breath detector. As illustrated in Fig. 8, breathing cycles of 45 year aged individual is recorded with two different types of breathing. One with normal breathing with nose and other with deeply inhaling and exhaling with mouth. When it is a normal breathing the initial resistance of the sensor was 80 M Ω , which reduced to 23 M Ω . The response time and recovery time were found to be 500 ms and 555 ms respectively. Similarly, for deep inhale–exhale pattern with mouth, the resistance changes from 58 M Ω to 1.4 M Ω with response and recovery time of 1 s and 5 s respectively. Thus, this breath sensor is extremely simple, yet very sensitive and would be very useful in the practical applications.

3.1 Humidity sensing mechanism

Sensing mechanism for humidity and breath sensing are similar. Here the principle of humidity sensing is based on the change of electrical resistance of the sensing material as a result of exposure to moisture.³² The humidity sensing mechanism can be explained by Grotthuss chain mechanism³³ (Fig. 9). The Au surface on exposure to humidity, chemisorbed water molecule forming hydroxyl species. As the humidity increases, water molecules get physisorbed on initially chemisorbed hydroxyl species through hydrogen bonding. More is the humidity, more is the formation of chains of physisorbed water molecules. Proton hopping between adjacent aqua molecules forms series of dipoles which can conduct charge easily. Hence, the sharp change of conductance/resistance and consequent high sensitivity can be observed in this region.

As the humidity increases, number of layers of hydroxyl group being adsorbed increases weakening the electrostatic force between the chemisorbed layer and the physisorbed layer. Hence, less hydronium ions are released and small change is detected in the resistance resulting in smaller sensitivity in higher humid region.

3.2 Breath sensing mechanism

Breath sensing mechanism is similar to the humidity sensing mechanism. In breathing, inhaling and exhaling processes are





4. Conclusions

in breath analysis. It would also be possible to make a wearable device using gold nanowires.

Conflicts of interest

There is no conflict of interest to report.

Acknowledgements

SK thanks Indian National Science Academy, New Delhi, India for its financial support through grant Scientist program, INSA Sanction No. SP/SS/216/1318.

References

- 1 L. Videman, B. P. Khanal and E. R. Zubarev, Functional gold nanorods: synthesis, self-assembly, and sensing applications, *Adv. Mater.*, 2012, **24**, 4811–4841.
- 2 D. G. Kotsifaki, M. Kandyla and P. G. Lagoudakis, Plasmon enhanced optical tweezers with gold-coated black silicon, *Sci. Rep.*, 2016, **6**, 26275.
- 3 X. Zhou, W. Xu, G. Liu, D. Panda and P. Chen, Size-dependent catalytic activity and dynamics of gold nanoparticles at the single-molecule level, *J. Am. Chem. Soc.*, 2010, **132**, 138–146.
- 4 Y. C. Yeh, B. Creran and V. M. Rotello, Gold nanoparticles: preparation, properties, and applications in bionanotechnology, *Nanoscale*, 2012, **6**, 1871–1880.
- 5 D. L. Feldheim and C. A. Fross, *Metal Nanoparticles*, Taylor & Francis Group, 2001.
- 6 H. Farahani, R. Wagiran and M. N. Hamidon, Humidity sensors principle, mechanism, and fabrication technologies: A comprehensive review, *Sensors*, 2014, **14**, 7881–7939.
- 7 M. A. Najeeb, Z. Ahmad and R. A. Shakoar, Organic thin-film capacitive and resistive humidity sensors: A focus review, *Adv. Mater. Interfaces*, 2018, 1800969.
- 8 V. Khambalkar, S. Birajdar, P. Adhyapak and S. Kulkarni, Nanocomposite of polypyrrol and silica rods-gold nanoparticles core-shell as an ammonia sensor, *Nanotechnology*, 2019, **30**, 105501.

- 9 Y. Zhang, W. Chu, A. D. Foroushani, H. Wang, D. Li, J. Liu, C. J. Barrow, X. Wang and W. Yang, New gold nanostructures for sensor applications: A review, *Materials*, 2014, **7**, 5169–5201.
- 10 F. Ratto, P. F. Rossi, L. Menabuoni, N. Tiwari, S. Kulkarni and R. Pini, Photothermal effects in connective tissues mediated by laser-activated gold nanorods, *Nanomedicine*, 2009, **5**, 143–151.
- 11 S. Zeng, K.-T. Yong, I. Roy, X.-Q. Dinh, X. Yu and F. Luan, A review on functionalized gold nanoparticles for biosensing applications, *Plasmonics*, 2011, **6**, 491–506.
- 12 J. B. Vines, J. H. Yoon, N. E. Ryu, D. J. Lim and H. Park, Gold nanoparticles for photothermal cancer therapy, *Front. Chem.*, 2019, **7**, 167.
- 13 C. Y. Lee and G. B. Lee, Humidity Sensors: A Review, *Sens. Lett.*, 2005, **3**, 1–14.
- 14 Z. Chen and C. Lu, *Sens. Lett.*, 2005, **3**, 274–295.
- 15 P. Adhyapak, R. Aiyer, S. R. Dugasani, H. U. Kim, C. KilSong, A. Vinu, V. Renugopalakrishnan, S. H. Park, T. Kim, H. Lee and D. Amalnerkar, Thickness-dependent humidity sensing by poly(vinyl alcohol) stabilized Au-Ag and Ag-Au core-shell bimetallic nanomorph resistors, *R. Soc. Open Sci.*, 2018, **5**, 171986.
- 16 Z. Duan, Q. Zhao, S. Wang, Q. Huang, Z. Yuan, Y. Zhang, Y. Jiang and H. Tai, Halloysite nanotubes: Natural, environmental-friendly and low-cost nanomaterials for high-performance humidity sensor, *Sens. Actuators, B*, 2020, **317**, 128204.
- 17 R. A. Shaikat, M. U. Khan, Q. M. Saqib, M. Y. Chougale, J. Kim and J. Bae, All range highly linear and sensitive humidity sensor based on 2D material TiSi₂ for real-time monitoring, *Sens. Actuators, B*, 2021, **345**, 130371.
- 18 Y. Huang, C. Liang, D. Wu, Q. Chang, L. Liu, H. Liu, X. Tang, Y. He and J. Qiu, Surface Ligand Engineering for a Lead-Free Cs₃Cu₂Br₅ Microcrystal-Based Humidity Sensor with a Giant Response, *J. Phys. Chem. Lett.*, 2021, **12**(13), 3401–3409.
- 19 Z. Zhen, Z. Li, X. Zhao, Y. Zhong, L. Zhang, Q. Chen, T. Yang and H. Zhu, Formation of uniform water microdroplet on wrinkled graphene for ultrafast humidity sensing, *Small*, 2018, **8**, 1703848.
- 20 C. H. Su, H. L. Chiu, Y. C. Chen, M. Yesilmen, F. Schulz, B. Ketelsen, T. Vossmeier and Y. C. Liao, Highly responsive PEG/gold nanoparticle thin-film humidity sensor via inkjet printing technology, *Langmuir*, 2019, **35**, 3256–3264.
- 21 I. Ali, L. Chen, Y. Huang, L. Song, X. Lu, B. Liu, L. Zhang, J. Zhang, L. Hou and T. Chen, Humidity-Responsive Gold Aerogel for Real-Time Monitoring of Human Breath, *Langmuir*, 2018, **34**, 4908–4913.
- 22 H. Feng, Y. Yang, Y. You, G. Li, J. Guo and T. Yu, Simple and rapid synthesis of ultrathin gold nanowires, their self-assembly and application in surface-enhanced Raman scattering, *Chem. Commun.*, 2009, 1984–1986.
- 23 L. H. Pei, K. Mori and M. Adachi, Formation process of two-dimensional networked gold nanowires by citrate reduction of AuCl₄[−] and the shape stabilization, *Langmuir*, 2004, **20**, 7837–7843.
- 24 H. Liu, X. Cao, J. Yang, X. Qing Gong and X. Shi, Dendrimer-mediated hydrothermal synthesis of ultrathin gold nanowires, *Sci. Rep.*, 2013, **3**, 3181–3187.
- 25 X. Lu, M. S. Yavuz, H. Y. Tuan, B. A. Korgel and Y. Xia, Ultrathin gold nanowires can be obtained by reducing polymeric strands of oleylamine-AuCl complexes formed via aurophilic interaction, *J. Am. Chem. Soc.*, 2008, **130**, 8900–8901.
- 26 A. Halder and N. Ravishanker, Ultrafine single-crystalline gold nanowire arrays by oriented attachment, *Adv. Mater.*, 2007, **19**, 1854–1858.
- 27 C. E. Cross, J. C. Hemminger and R. M. Penner, Physical vapor deposition of one-dimensional nanoparticle arrays on graphite: Seeding the electrodeposition of gold nanowires, *Langmuir*, 2007, **23**, 10372–10379.
- 28 X. Gao, F. Lu, B. Dong, Y. Liu, Y. Gao and L. Zheng, Facile synthesis of gold and gold-based alloy nanowire networks using wormlike micelles as soft templates, *Chem. Commun.*, 2015, **51**, 843–846.
- 29 K. P. Yoo, L. T. Lim, N. K. Min, M. J. Lee, C. J. Lee and C. W. Park, Novel resistive-type humidity sensor based on multiwall carbon nanotube/polyimide composite films, *Sens. Actuators, B*, 2015, **145**, 120–125.
- 30 D. Barmpakos, A. Segkos, C. Tsamis and G. Kaltsas, A disposable flexible humidity sensor directly printed on paper for medical applications, *J. Phys.: Conf. Ser.*, 2017, **931**, 012003.
- 31 M. A. Squillaci, M. A. Stoeckel and P. Samori, 3D hybrid networks of gold nanoparticles: mechanoresponsive electrical humidity sensors with on-demand performances, *Nanoscale*, 2019, **11**, 19319–19326.
- 32 S. Gong, W. Schwalb, Y. Wang, Y. Chen, Y. Tang, J. Si, B. Shirinzadeh and W. Cheng, A wearable and highly sensitive pressure sensor with ultrathin gold nanowires, *Nat. Commun.*, 2014, **5**, 3132.
- 33 N. Agmon, The Grotthuss mechanism, *Chem. Phys. Lett.*, 1995, **244**(56), 456–462.
- 34 R. Buchhold, A. Nakladal, G. Gerlach and P. Neumann, Design studies on piezoresistive humidity sensors, *Sens. Actuators, B*, 1998, **53**, 1–7.
- 35 C. Stenner, L. H. Shao, N. Mameka and J. Weissmüller, Piezoelectric gold: strong charge-load response in a metal-based hybrid nanomaterial, *Adv. Funct. Mater.*, 2016, **26**, 5174–5181.
- 36 N. Yadav, P. Chaudhary, K. K. Dey, S. Yadav, B. C. Yadav and R. R. Yadav, Non-functionalized Au nanoparticles can act as high-performing humidity sensor, *J. Mater. Sci.: Mater. Electron.*, 2020, **31**(20), 17843–17854.
- 37 S. Gong, W. Schwalb, Y. Wang, Y. Chen, Y. Tang, J. Si, B. Shirinzadeh and W. Cheng, A wearable and highly sensitive pressure sensor with ultrathin gold nanowires, *Nat. Commun.*, 2014, **5**(1), 1–8.

